Near-field Seismic Design Motions: A Case Study From Wellington, New Zealand

J.B. Berrill
Reader, University of Canterbury, New Zealand

Summary The special character of ground shaking close to the fault together with the difficulty of theoretical predictions requires that near-field design motions be estimated empirically. However, the set of near-field strong motion records is far from complete, and scaling must be employed in most cases. Simple rules for scaling near-field records are reviewed and illustrated with an example from Wellington, New Zealand.

1. INTRODUCTION

The enormous loss of life and damage to Kobe and the surrounding Hanshin district from the M7.2 Hyogo-ken Nambu earthquake of 17 January 1995 illustrates the devastation that can occur in the epicentral region of a moderate (in terms of magnitude) earthquake in a modern, intensely urbanized area. Thus, the estimation of ground motions in the near field of faults is surely an appropriate topic within the conference theme of *Geomechanics in a Changing World.*

The problem of estimating near-field design motions, roughly those which occur within one source width of the rupture, is a difficult one. The rupture cannot be idealized as a point source, and higher order components of seismic radiation such as those which attenuate as $1/r^2$ (where r is distance) and which can be ignored at greater distances are important in the near field. Furthermore, ground displacements carried by these components are directly proportional to fault displacement rather than to its derivative as are the components which attenuate as $1/r$ and dominate in the far field. Thus the character of near-field shaking is different from that of far-field motion and cannot properly be obtained by extrapolation. Moreover, since the higher order terms are relatively rich in long-period components of motion than the $1/r$ terms, scaling of an average far-field spectrum according to peak acceleration is inappropriate. The special character of near-field motions, which may be further modified by directivity effects, demands that they be estimated independently.

How can this be done? The mechanics of a propagating shear dislocation are well understood. But analytical solutions, as well as being difficult, are highly dependent on details of stress field, rock properties and fault geometry as well as conditions at the site. This suggests that an empirical approach be taken, using records of actual near-field motions obtained in similar conditions to those of the site under study. But the number of recordings made close to the source is quite small and far from complete. However, this difficulty can be overcome by using theoretical results to scale existing accelerograms for magnitude, gross mechanism (thrust, normal or strike slip) and gross recording site properties. In this way, a set of near-field records, scaled to match the gross properties of the fault and site of interest, can be assembled.

In this paper, scaling relationships for response spectra are presented and then applied to a site in Wellington, New Zealand, 400 m from the Wellington Fault, one of the main expressions in central New Zealand of the boundary between the Pacific and Indian plates. The scaling rules are not original, but they have appeared mainly in the seismological literature. The example used is taken from a study by the author for the strengthening of the New Zealand Parliament Buildings, made in 1990. Hence the records used do not include the several near-field accelerograms obtained since then, for example in the 1994 Northridge, California and 1995 Hyogo-ken Nambu, and other recent Japanese earthquakes.

2. SCALING LAWS

Consider a site close to a fault whose general rupture characteristics are known; i.e.. we know the magnitude of the *characteristic* event and the general mechanism (strike slip, normal or thrust). Suppose also that we know the gross site characteristics, described by wave velocity and density profiles. Three principal scalings are described below to adjust existing records to the case of interest. These are for magnitude, source mechanism and gross site effects.

2.1 Magnitude Scaling

Magnitude effects are markedly dependent on frequency. High-frequency components of motion depend principally on rupture of the closest section of the fault, and so are little influenced by the overall magnitude of the event. Long-period components, on the other hand, are determined by a

much larger portion of the rupture surface and hence depend more strongly on magnitude. From Boore and Joyner (1982), ground motion y may be scaled for magnitude M from event 1 to 2 according to the following relationship:

$$\log\left(\frac{y_1}{y_2}\right) = b(M_1 - M_2) + c\left[(M_1 - 6)^2 - (M_2 - 6)^2\right] \quad (1)$$

When y represents pseudo velocity response with 5% damping, b and c take the values given in Table 1.

Table 1. Parameters of Joyner and Boore (1982) for scaling pseudo velocity response at 5% damping.

Period (sec)	b	c
0.1	0.25	- 0.06
0.15	0.30	- 0.08
0.2	0.35	- 0.09
0.3	0.42	- 0.11
0.4	0.47	- 0.13
0.5	0.52	- 0.14
0.75	0.60	- 0.16
1.0	0.67	- 0.17
1.5	0.74	- 0.19
2.0	0.79	- 0.20
3.0	0.85	- 0.22
4.0	0.88	- 0.24

2.2 Scaling for Source Mechanism

Source characteristics such as stress drop, fault roughness or coherence length, directivity and radiation pattern all affect the strength of shaking, but at present we have little chance of predicting these effects. However, we can correct for average differences in radiation pattern between thrust, strike-slip and normal faulting mechanisms. Boore and Boatwright (1984) have calculated average radiation coefficients for various ranges of take-off angles, corresponding to teleseismic, regional and close distances. In the Wellington example below, we have used values from their Table 5 (close distances) to adjust thrust and oblique-slip records to the strike-slip motion expected on the Wellington Fault. The values for SH waves are given in Table 2.

2.3 Gross Site Effects

Incoming seismic waves may undergo local modification, *site effects*, in the vicinity of the site due to marked variations in geometry and material properties near and at the ground surface. Site effects have several causes: focusing of rays due to topographic or subsurface irregularities; resonance in near-surface layers; attenuation, particularly of high-

Table 2. Average absolute value of radiation pattern F for SH waves close to source, from Boore and Boatwright (1984), for various source mechanisms.

Mechanism	$\langle \lvert F \rvert \rangle$
Vertical, strike slip	0.39
30° dip, dip-slip	0.29
45° dip, oblique-slip	0.34

frequency components; and amplification due to a decrease in acoustic impedance towards the surface. In general, geometric and topographic effects are not as important as material ones. Resonance effects may be important where there are unusually soft layers in the upper few tens of metres, and these can be treated by a conventional site analysis.

In the Parliament study, the site is on firm ground and resonance effects are not considered. In this example and in many cases, the major effect is one of amplification due to a general reduction in impedance, $I = \sqrt{\rho c}$, where ρ = mass density and c = wave velocity. This effect can be thought of from the point of view of energy conservation. As waves pass from an underlying dense, stiff material into a softer, less dense material, greater deformations and particle velocities (i.e., greater wave amplitudes) are required for seismic energy density to be conserved. Thus incoming waves are progressively amplified as they pass into softer near-surface rock and soils.

Joyner and Fumal (1984) suggested that a first approximation for this effect could be made by considering the shear-wave impedance over a depth equal to the upper quarter wave length at the period under consideration. Between the centre of energy release and the ground surface, we construct an *impedance factor* F_i such that

$$F_i = \sqrt{\frac{\rho_c \beta_c}{\rho_{av} \beta_{av}}} \quad (2)$$

where ρ_c, β_c are density and shear wave velocity of the rock at the centre of energy release, and ρ_{av} and β_{av} are density and shear wave velocity averaged from the upper quarter wavelength of travel path. This factor is then used to adjust for the gross variation in impedance along the wave path.

3. APPLICATION TO PARLIAMENT SITE

Seismic hazard at Parliament Buildings and indeed for most of the metropolitan Wellington area, is dominated by the Wellington Fault which passes within 400 m of the site. Geological investigations show about 100 m of strike-slip post-glacial offset, with an apparent characteristic event with around 4 m offset and a rupture length of about 80 km

starting at Cook Strait and running northwards, corresponding to a magnitude in the range of 7 to 7½ (Van Dissen *et al.*, 1992). Dating of events suggests that the next rupture is likely to occur within a few hundred years. Such a rupture clearly marks the design event for the Parliament strengthening. The problem, then, is to find a set of near-field records representing motions from a magnitude 7 to 7½ earthquake with a strike-slip mechanism, and recorded on fairly firm ground. In 1990, when the strengthening works were designed, there was only one record with those characteristics. Therefore, the procedures described above were employed to scale additional records.

3.1 Near Field Accelerograms

A set of nine of the strongest near-field records available in 1990 is listed in Table 3 together with the corresponding earthquake parameters in Table 4. Response spectra for these records are plotted in Figures 1 and 2.

Notice that the thrust events are stronger at high frequencies (short periods) and also flatter in the mid and long period band than the strike-slip motions, except for the 1979 El Centro array records which are possibly influenced a moderate amount by bifucation of the rupture near the instrument sites (Archuleta, 1982).

For preliminary design work, a "design" curve was sketched somewhat arbitrarily through the unmodified spectra in Figures 1 and 2, as shown in Figure 3. It runs near the upper limit of the observed spectra because for this particular structure base isolation was chosen for the strengthening and such systems do not tolerate overloads.

For time-history analyses of the strengthened structure, a set of four records was chosen comprising El Centro, 1979 No. 6; Corralitas 1989; and Gazli, 1976 which were scaled to represent an M7½ event on the Wellington Fault, together with the Llolleo, Chile, 1985 record representing a subduction rupture beneath the city. Corralitos was chosen because it had the largest magnitude amongst the strike-slip records; El Centro No. 6 for its strength and Gazli for its large magnitude.

3.2 Scaling of Selected Records

Adjusting for magnitude is straight-forward, using (1) and the coefficients from Table 1. Since the 1979 Imperial Valley earthquake had a strike slip mechanism, no mechanism adjustment is required for the El Centro No. 6 record. For Gazli, the factor F_{mech} = 0.39/0.29 = 1.345 is applied, where 0.39 and 0.29 are the average pattern values from Table 2

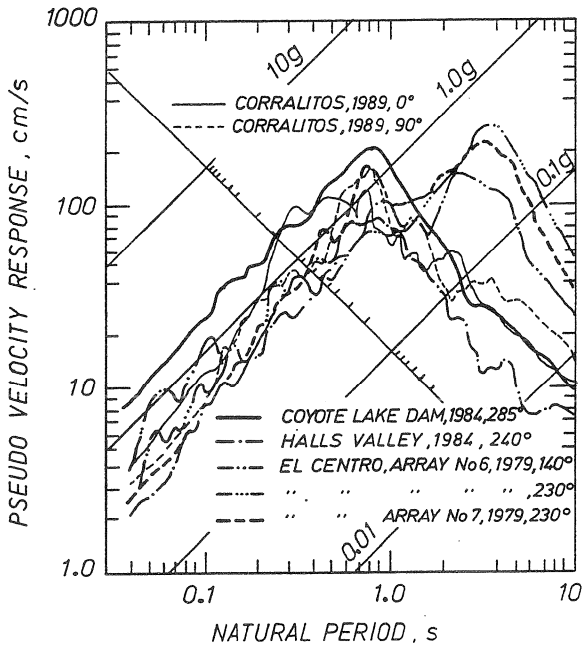

Figure 1. Response spectra from strike-slip events. Damping is 5%.

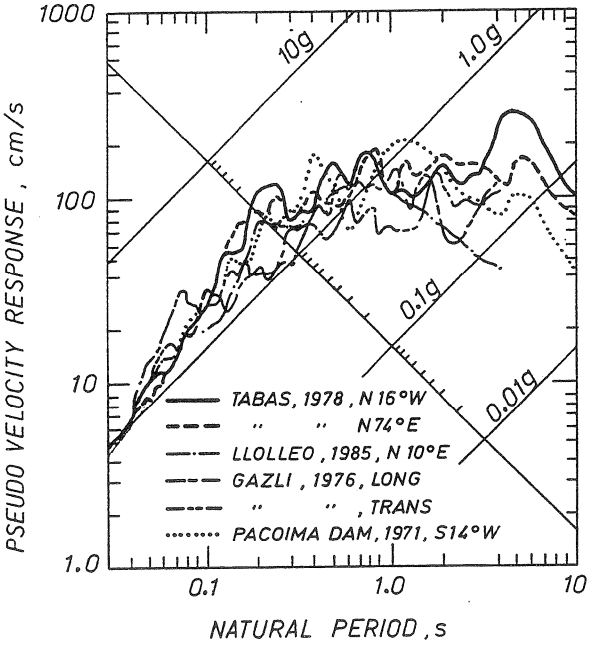

Figure 2. Response spectra from thrust and subduction events. Damping is 5%.

for strike-slip and thrust (dip-slip) mechanisms respectively. In the Loma Prieta rupture, the slip was not purely strike-slip but also had an oblique component on a surface dipping at about 70°. We have roughly approximated this by averaging the factors for oblique slip on a 45° dipping surface and for pure strike-slip, to get for the Corralitas record

$$F_{mech} = \frac{1}{2}(1 + 1.147) = 1.074.$$

Table 3. Strong, near field accelerograms (available before 1990).

Earthquake	Magnitude M_s	Site	Distance to Fault km	Component	Peak Acceleration g	Site Conditions
Strike Slip Events						
Imperial Valley, Ca 15 October 1979	6.5	El Centro Array No 6	1	140° 230° up	0.37 0.43 1.66	Sediments, 4-5 km deep Velocity and density profile given by Olsen and Apsel, (1982)
		El Centro Array No 7	1	140° 230° up	0.33 0.45 0.50	
		Bonds Corner	3	140° 230° up	0.58 0.77 0.35	
Morgan Mill, Ca 24 April 1984	6.1	Coyote Dam Abutment	< 3	195° 285° up	0.71 1.30 0.40	
		Halls Valley	< 3	150° 240° up	0.15 0.31 0.11	
Loma Prieta, Ca 18 October 1989	7.1	Corralitos	< 1	90° 360° up	0.50 0.64 0.47	Shallow landslide debris over rock J.C. Tinsley, pers. comm.
Thrust Events						
Tabas, Iran 16 September 1978	7.4	Tabas	3	N74°E N16°E V	0.86 0.92 0.72	Alluvium (Hadley *et al.*, 1983)
Gazli, USSR 17 May 1976	7.1	Gazli		N-S E-W V	0.60 0.71 1.32	1400 m interbedded sandstone and clay, overlying schist (Hartzell, 1980)
Coalinga, Ca 2 May 1983	6.5	Pleasant Valley Pump Station		45° 135° up	0.59 0.52 0.47	150 m alluvium over 10 km sedimentary rock (Jarpe *et al.*, 1988)
San Fernando, Ca 9 February 1971	6.6	Pacoima Dam		S14°W N76°W V	1.15 1.06 0.70	Crystaline basement rock near crest of ridge (Trifunac and Hudson, 1971)
Nahanni, Canada 23 December 1985	6.9	Iverson		280° 10° V	1.35 1.10 2.37	Basement rock Weidcher *et al.*, (1986), Wetmiller *et al.*, (1988)
Subduction Event						
Valparaiso, Chile 3 March 1985	7.8	Llolleo		N10°E S80°E V	0.67 0.43 0.85	Sandstone and volcanic rock (Wyllie *et al.*, 1986)

Table 4. Earthquake Parameters.

Earthquake	Date	Magnitude M_s	$M_O \times 10^{18}$ N-m	Mechanism*	Depth km	Rupture Length km	Rupture Width km	Offset m	Reference
Imperial Valley, Ca	15 Oct	6.5	6.0	S		42	10	0.80	1,2
Morgan Hill, Ca	24 Apr 84	6.1	2.0	S		30	10		1
Loma Prieta, Ca	18 Oct 89	7.1	22-38	O	17.6	~45	~14	1.9 h 1.3 rev	3
San Fernando, Ca	9 Feb 71	6.6	12	T	15	17	17	2.1	1
Gazli, USSR	17 May 76	7.1	21	T	10	30		3.3	2,8,9,10
Tabas, Iran	16 Sept 78	7.4	15	T	10.5	65	~20	1.5	1,2,4
Coalinga, Ca	2 May 83	6.5	2.5	T					5,6
Valparaiso, Chile	3 Mar 85	7.8	115	SUBD		170	100	1.6	7
Nahanni, Canada	23 Dec 85	6.9	15-18	T		25	15	1.3	11,12

* S = Strike slip
O = Oblique
T = Reverse thrust
SUBD = Subduction

1. Kanamori and Allen, (1986)
2. Ambraseys and Menu, (1988)
3. USGS Staff, (1990)
4. Niazi and Kanomori, (1981)
5. Pearson, (1984)
6. Uhrhammar *et al.*, (1984)
7. Kausel, (1985)
8. Hartzell, (1980)
9. Kristy *et al.*, (1980)
10. Aptekman *et al.*, (1989)
11. Choy and Boatwright, (1988)
12. Wetmiller *et al.*, (1988)

Allowing for site impedance is a little more complex. First, velocity profiles for the sites are found from the literature. Density profiles could not be found for all sites. However, since density varies much less than wave velocity, this is not a serious handicap.

The profiles are given in Tables 5 through 7. No profile could be found for Corralitos, so it was assumed identical to Wellington. Using these profiles shear wave velocities averaged over the upper quarter wavelength were found by trial and error for selected natural periods. For the Wellington site, for example, the quarter wavelength value varied from 64 m at a period of 0.1 sec to 3.08 km at 4.0 sec. Then impedance factors were computed using (2). The results are listed in Table 8.

Finally, overall scaling factors were calculated. For record j, the scaling factor S_j is:

$$S_j(T) = F_{mag}(T)_j \times F_{mech\,j} \times F_i(T)_{Wgtn} / F_i(T)_j \quad (3)$$

Using (3) the scaling factors shown in Table 9 were computed. The scaled pseudo velocity spectra are shown in Figure 3.

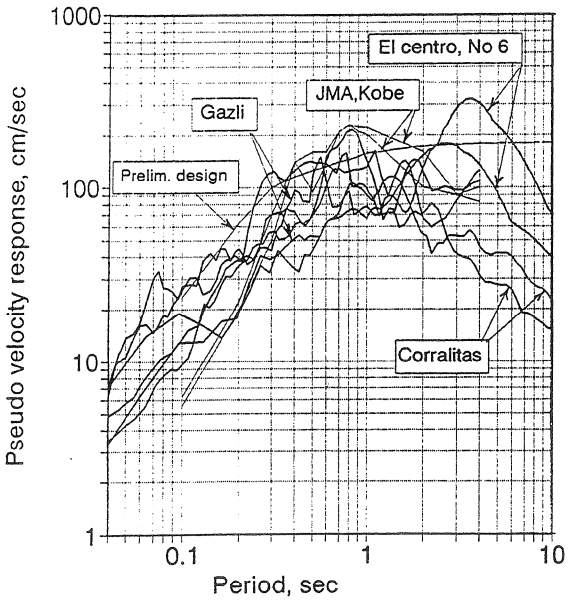

Figure 3. Spectra of the sealed horizontal motions. Note the generally good agreement with the Kobe record.

4. CONCLUSION

Until a more complete set of records is available, the procedures illustrated here provide a rational way of scaling near-field earthquake accelerograms for design of structures close to (say within 10 to 15 km) active faults.

Table 5. Shear wave velocity profile for Wellington (Robinson, 1986).

Depth, km	β, km/sec
0 - 0.4	2.54
0.4 - 5.0	3.16
5 - 15	3.49

Table 6. Shear wave velocity and density profile for the Gazli site (Hartzell, 1980).

Depth, km	β, km/sec	ρ, t/m^3
0 - 1.4	1.44	2.10
1.4 - 12	3.41	2.20
12 - 25	3.52	2.80

Table 7. Profile at El Centro site (from Olson and Apsel, 1982).

Depth, km	β, km/sec	ρ, t/m^3
0 - 0.10	0.50	2.04
0.10 - 0.25	0.818	2.06
0.25 - 0.75	1.010	2.13
0.75 - 1.25	1.200	2.21
1.25 - 1.75	1.410	2.28
1.75 - 2.25	1.620	2.35
2.25 - 2.75	1.850	3.43
2.75 - 3.25	2.080	2.50
3.25 - 3.75	2.330	2.57
3.75 - 4.25	2.590	2.65
4.25 - 4.75	2.870	2.72
4.75 - 5.25	3.060	2.77
5.25 - 5.75	3.32	2.85
5.75 - 11.0	3.87	3.04

Table 8. Impedance factors derived from site profiles.

Period, sec	Wellington $F_i = \frac{\sqrt{3.49}}{\beta_{av}}$	El Centro No. 6 $F_i = \frac{\sqrt{3.32 \times 2.85}}{\beta_{av}\ \rho_{av}}$	Gazli $F_i = \sqrt{\frac{3.41 \times 2.70}{1.44 \times 2.10}}$
0.1	1.17	3.05	
0.2	1.17	3.05	
0.5	1.17	3.05	= 1.745
1.0	1.11	2.80	for all
2.0	1.08	2.37	periods
3.0	1.07	2.25	
4.0	1.06	2.14	

Table 9. Overall scaling factors.

Period, sec	El Centro 1979, No. 6	Corralitas 1989	Gazli 1976
0.1	0.52*	1.17	0.98*
0.2	0.57*	1.20	1.00
0.5	0.67*	1.24	1.04
1.0	0.89*	1.36	1.08
2.0	1.12	1.38	1.07
3.0	1.22	1.39	1.06
4.0	1.24	1.36	1.03

* Replaced by 1.0

REFERENCES

Ambraseys, N.N. and Menu, J.M. (1988). Earthquake-Induced Ground Displacements, *Earthq. Eng.* and *Struct Dyn.* Vol. 16, pp. 985-1006.

Aptekman, J., Arefiev S., Afimiina, T., Aleksin, P., Borissoff, B., Graizer, B., Molotkov, S., Pietnev, K., Shebalin, N., Shilova, N., Shteinberg, V., Tatevosyan, R. (1989). Epicentral Seismological Observations following Disastrous Earthquakes, *Unpublished report*, Epicentral Seismological Expedition, Institute of Physics of Earth, Moscow.

Archuleta, R.J. (1982). Analyses of Near-Source Static and Dynamic Measurements from the 1979 Imperial Valley Earthquake, *Bull. Seism. Soc. Am.*, Vol. 72, pp. 1927-1956.

Boore, D.M. and Boatwright, J. (1984). Average Body-Wave Radiation Coefficients, *Bull. Seis. Soc. Am.*, Vol. 74, pp. 1615-1622.

Choy, G.L. and Boatwright, J. (1988), Teleseismic and Near-Field Analysis of the Nahanni Earthquakes in the Northwest Territories, Canada, *Bull. Seism. Soc. Am.*, Vol. 78, pp. 1627-1652.

Hadley, D.M., Hawkins, H.G. and Benuska, K.L. (1983). Strong Ground Motion Record of the 16 September 1978 Tabas, Iran, Earthquake, *Bull. Seism. Soc. Am.*, Vol. 73, pp. 315-320.

Hartzell, S. (1980). Faulting Process of the May 17, 1976 Gazli, USSR Earthquake, *Bull. Seism. Soc. Am.*, Vol. 70, pp. 1715-1736.

Jarpe, S.P., Cramer, C.H., Tucker, B.E., and Shakal, A.F. (1988). A Comparison of Observations of Ground Response to Weak and Strong Ground Motion at Coalinga, California, *Bull. Seism. Soc. Am.*, Vol. 78, pp. 421-435.

Joyner, W.B. and Fumal, T.E. (1984). Use of Measured Shear-Wave Velocity for Predicting Geologic Site Effects on Strong Ground Motion, *Proc. Eighth World Conf. Earthq. Eng.*, Vol. 2, pp. 777-783.

Joyner, W.B. and Boore, D.M. (1982). Prediction of Earthquake Response Spectra, *U.S. Geol. Surv. Open-File Report 82-977*, 16p.

Kanamori, H. and Allen, C.R. (1986). Earthquake Repeat Times and Average Stress Drop, *Earthquake Source Mechanics*, Geophysical Monograph 37, Am. Geophys Union, pp. 227-236.

Kausel, E. (1985). Proceso Sismieco, Parametros Focales y Replicas del Sismo del 3 de Marzo, 1985, in *El Sismo de Marzo 1985, Chile*, University of Chile, pp. 31-41.

Kristy, M.J., Burdick, L.J. and Simpson, D.W. (1980). The Focal Mechanisms of the Gazli, USSR, Earthquake, *Bull. Seism. Soc. Am.*, Vol. 70, pp. 1737-1750.

Niazi, M. and Kanamori, H. (1981). Source parameters of 1978 Tabas and 1979 Qainat, Iran, earthquakes from long-period surface waves, *Bull. Seism. Soc. Am* Vol. 71, pp. 1201-1213.

Olson, A.H. and Apsel, R.J. (1982). Finite Faults and Inverse Theory with Applications to the 1979 Imperial Valley Earthquake, *Bull. Seism. Soc. Am.*, Vol. 72, pp. 1969-2012.

Pearson, W.J. ed. (1984). Seismological Notes, *Bull. Seism. Soc. Am.*, Vol. 74, pp. 785-789.

Robinson, R. (1986). Seismicity, Structure and Tectonics of the Wellington Region, New Zealand, *Geophy. J. R. Astr. Soc.*, Vol. 87., pp. 379-409.

Trifunac, M.D. and Hudson, D.E. (1971). Analysis of Pacoima Dam Accelerogram – San Fernando, California Earthquake of 1971, *Bull. Seism. Soc. Am.*, Vol. 61, pp. 1393-1411.

Uhrhammer, R.A., Darragh, R.B. and Bolt, B.A. (1984). The 1983 Coalinga Earthquake Sequence: May 2 through August 1 in EERI Report No. 84-03, pp. 9-17.

USGS Staff (1990). The Loma Prieta, California Earthquake: An Anticipated Event, *Science*, Vol. 247, pp. 286-293.

Van Dissen, R.J., Berryman, K.R., Pettinga, J.R. and Hill, N.L. (1992). Paleoseismicity of the Wellington-Hutt Valley Segment of the Wellington Fault, North Island, New Zealand, N.Z. J. Geol. Geophys., Vol. 35, pp. 165-176.

Weichert, D.H., Wetmiller, R.J. and Munro, P. (1986). Vertical Earthquake Acceleration Exceeding 2g?, *Bull. Seism. Soc. Am.*, Vol. 76, pp. 1473-1478.

Wetmiller, R.J. *et al.* (1988). An analysis of the 1985 Nahanni Earthquakes, *Bull. Seism. Soc. Am.*, Vol. 78, pp. 590-616.

Wyllie, L.A. *et al.* (1986). The Chile Earthquake of March 3, 1985 – Seismological Features, *Earthquake Spectra*, Vol. 2, pp. 253-272.